JACS
JOURNAL OF THE AMERICAN CHEMICAL SOCIETY
Communication
pubs.acs.org/JACS

Non-innocent Dissociation of H_2O on GaP(110): Implications for Electrochemical Reduction of CO_2

Ana B. Muñoz-García[†,‡] and Emily A. Carter*[,‡,§]

[†]Department of Chemical Sciences, University of Naples Federico II, Via Cintia, 80126 Naples, Italy

[‡]Department of Mechanical and Aerospace Engineering and [§]Program in Applied and Computational Mathematics and the Andlinger Center for Energy and the Environment, Princeton University, Princeton, New Jersey 08544-5263, United States

Supporting Information

ABSTRACT: The structural and electronic properties of the GaP(110)/H_2O interface have been investigated by first-principles density functional theory calculations. Our results suggest that hydride-like H atoms are present on the surface as a consequence of the dissociation of water in contact with the GaP surface. This feature opens up a new feasible reduction pathway for CO_2 where the GaP(110) surface is the electrochemically active entity.

Recycling of CO_2 into usable fuels is a goal being pursued by scientists and engineers to tackle simultaneously the dramatically increasing atmospheric CO_2 levels and the eventual exhaustion of fossil fuel resources. Unfortunately, the great stability of the CO_2 molecule turns such transformations into a very challenging task and none of the processes developed to date have arrived at a commercial stage. The main drawbacks of the electrochemically-catalyzed reduction of CO_2 are high overpotentials (i.e., kinetic barriers), low current efficiency, and/or poor electrode stability. Moreover, the CO_2 reduction reaction is thermodynamically nonselective, so mixtures of reduced species (e.g., HCO_2H, H_2CO, CH_3OH) are typically obtained.[1] Bocarsly and co-workers reported a pyridinium-catalyzed reduction of CO_2 on p-GaP electrodes that overcomes the overpotential problem (driven by light only) as well as the lack of selectivity (high Faradaic yield of CH_3OH). However, the overall low efficiency remains a critical shortcoming of this promising reaction.[2,3] Several experimental and theoretical studies have been performed to clarify and eventually to improve this chemistry, but the underlying mechanism is not yet well understood. It was proposed initially to be a homogeneous process consisting of a series of one-electron shuttling steps, starting from the reduction of the pyridinum cation to form pyridinyl radical, which in turn acts to reduce CO_2 through an initial carbamate complex.[3,4] Some experimental observations, however, are inconsistent with this hypothesis. The fact that this conversion is electrode-dependent (occurs on Pd,[4] Pt,[3,5] and p-GaP[2] electrodes but not on glassy carbon without addition of 4,4′ bypiridine[3]) and the saturation of the reaction kinetics above a given pyridinium concentration (8 mM)[5] hint at a surface-mediated process. Moreover, two recent independent theoretical studies (by Keith and Carter[6] and Tossell[7]) agree on assigning a reduction potential for the pyridinium cation in aqueous solution that is ∼1 V more negative than the experimental one (−1.37 V[6] and −1.44 V[7] vs −0.58 V[3], all vs SCE), which suggests that what is being measured is something other than a homogeneous reduction of pyridinium, with reduction of a surface-bound species being an obvious candidate.

These findings motivated us to focus our research on the p-GaP electrode in an attempt to clarify its role in the CO_2 reduction reactions. Since electrochemical processes frequently occur in aqueous environments, an understanding of electrode/water interface features is a prerequisite when it comes to rationalizing surface and electrochemical phenomena. Thus, in this work we characterize the structural, energetic, and electronic features of the GaP(110)/H_2O interface by performing periodic all-electron, frozen-core, projector-augmented-wave (PAW)[8] density functional theory (DFT)[9] calculations. We used the Perdew–Burke–Erzenhof (PBE)[10] generalized gradient approximation exchange–correlation functional and standard PAW electron–ion potentials as implemented in the VASP code (version 5.2.2).[11] Our model system was a seven-layer slab of a 1 × 2 unit cell of GaP(110) containing four GaP formula units per layer. This slab was generated by cleaving bulk GaP with the equilibrium lattice constant of 5.534 Å determined by DFT-PBE, which is 1.5% larger than the experimental one (5.45 Å[12]). Different coverages of water [from 0.25 to 5 monolayer (ML)] were modeled by addition of water molecules symmetrically above and below GaP(110) slabs so that no dipole corrections due to periodic images were needed. The H_2O/GaP(110) geometries were obtained by allowing full relaxation of all the H_2O molecules and the surface and neighboring subsurface atoms of the slab, keeping the three bulklike central layers frozen in the equilibrium bulk structure to mimic a semi-infinite bulk crystal. The vacuum region between periodic images of the H_2O/GaP(110) slab was always >16 Å. A kinetic energy cutoff of 600 eV was used to converge the plane-wave basis. The **k**-point sampling used (4 × 3 × 1) was based on the Monkhorst–Pack scheme.[13] The Gaussian smearing method (with a smearing width of 0.01 eV) was used for integration of the Brillouin zone. These parameters provided convergence of the computed total energy to within 1 meV per formula unit. To analyze atomic charges, we employed Bader's topological partition of the electronic density.[14] Additional details are provided in the Supporting Information (SI).

Received: June 28, 2012
Published: August 8, 2012

   dx.doi.org/10.1021/ja3063106 | J. Am. Chem. Soc. 2012, 134, 13600–13603

The GaP/H_2O interface has not been examined experimentally to date. However, measurements indicate partial dissociation of H_2O on the analogous III−V GaAs(110) surface,[15,16] motivating us to consider both molecular and dissociative adsorption. We studied dissociation of isolated molecules of H_2O as well as degrees of dissociation from 25 to 100% of the first monolayer of H_2O for coverages (Θ) of 3, 4, and 5 ML, corresponding to one out of four up to four out of four dissociated molecules of H_2O on each 1 × 2 (110) side of the GaP slab. When necessary, we surveyed all possible relative positions of dissociated molecules of H_2O. Detailed information on the cases studied is provided in the SI. The transition states for H_2O dissociation were found using the climbing image nudged elastic band method.[17]

GaP is made p-type by doping with, for example, Zn to produce its electron deficiency. We therefore modeled p-GaP as Zn-doped GaP (Zn:GaP) by substituting some Ga atoms with Zn atoms (Zn_{Ga}). We predicte that segregation of Zn to the surface is increasingly favorable as the concentration of Zn decreases, so we expect some Zn to be present at the surface of p-GaP(110) (see the SI). We therefore also evaluated the chemical features of the H_2O/Zn:GaP(110) interface. In our model, one out of every four atoms of Ga at the surface was substituted by a Zn atom (i.e., $[Zn]_{Surf}$ = 25%). We find that this high concentration of Zn does not change the GaP(110)/H_2O interface features, and therefore, we restrict the discussion in the main text to the chemistry of water on pure GaP(110). Details concerning the Zn:GaP(110) surface and the Zn:GaP(110)/H_2O interface can be found in the SI.

The clean surface of GaP(110) has been widely studied and by now is well characterized;[18] our results are in complete agreement with reported experimental features. After cleavage, each Ga (P) of GaP(110) loses one of its four P (Ga) neighbors and, as in other III−V (110) surfaces, it relaxes in such a way that surface Ga atoms move inward and surface P atoms move outward. The driving force for this rearrangement is that under the coordination conditions of the surface, group-III atoms (Ga) prefer a planar sp^2-like environment while group-V atoms (P) accommodate their three neighbors in a pyramidal sp^3-like manner.[18c] The presence of surface Zn_{Ga} does not modify this relaxation pattern.

With this particular surface topography, the final structure and properties of the H_2O/GaP(110) interface depend on the resulting balance between water−surface and water−water interactions. We analyze these contributions by re-expressing the adsorption energy (E_{Ads}) of H_2O,

$$E_{Ads} = E_{S+W} - E_S^V - nE_{1W}^V$$

(where E_{S+W}, E_S^V, and E_{1W}^V are the energies of the total slab + water system, the bare slab, and one isolated molecule of H_2O, respectively, and n is the number of water molecules) as a sum of three terms:

$$E_{Ads} = (E_{S+W} - E_S - E_W) + (E_S - E_S^V) + (E_W - nE_{1W}^V)$$
$$= E_{S/W} + E_{S/S} + E_{W/W}$$

where E_S and E_W are the energies of the GaP(110) slab and water molecules frozen in the equilibrium geometry of the water/GaP interface, respectively. Expressed in this way, the first term, $E_{S/W}$, represents the electronic interaction between the slab and water layers; the second term, $E_{S/S}$, quantifies the energy change due to relaxation of the slab in contact with H_2O versus the slab in vacuum; and the third term, $E_{W/W}$, is the cohesive energy of the water molecules in their equilibrium structure at the interface. These three terms, along with E_{Ads}, are plotted in Figure 1a as functions of H_2O coverage, for the molecular adsorption of H_2O on GaP(110).

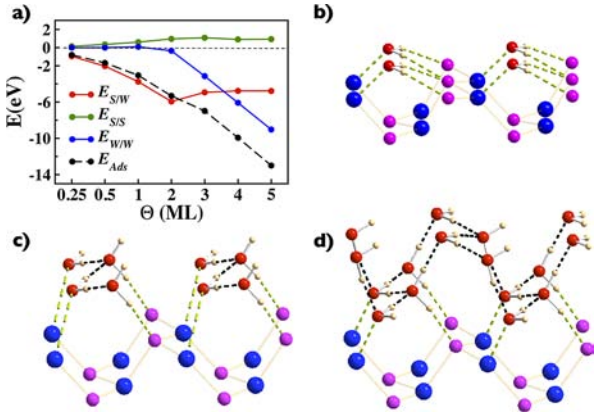

Figure 1. (a) Plots of the adsorption energy E_{Ads} and its three components for undissociated H_2O on GaP(110) as functions of water coverage Θ. (b−d) Predicted structures for the molecular adsorption of (b) 1, (c) 2, and (d) 4 ML of H_2O. Ga atoms are shown in blue, P atoms in fuchsia, O atoms in red, and H atoms in tan.

For low coverages (Θ < 2 ML), each molecule of H_2O maximizes its interaction with the surface by forming one Ga−O bond (an O lone pair donates into an empty Ga 4p orbital) and two P−H bonds (H bonds to the P lone pairs) (Figure 1b). No H_2O−H_2O interaction is predicted ($E_{W/W} \approx 0$), so E_{Ads} behaves as $E_{S/W}$. The turning point occurs at Θ = 2 ML, where two molecules of H_2O, connected by a H-bond, maximize their interaction with the surface by bridging a Ga−P pair (Figure 1c). For Θ > 2 ML, these Ga−OH_2−OH_2−P bridges are preserved and the added monolayers of H_2O create a network (Figure 1d). As a result, $E_{S/W}$ is maximized for Θ = 2 ML and becomes roughly constant beyond that coverage, with the adsorption energy for Θ > 2 ML determined instead by the increasingly negative $E_{W/W}$ term. A structural perturbation in the surface is induced by the presence of water for $\Theta \geq$ 2 ML (positive $E_{S/S}$ term), but this is small in comparison with the magnitude of the water−surface and water−water interactions.

Dissociative adsorption of H_2O on GaP(110) is considered next. For Θ < 2 ML (i.e., with noninteracting molecules of H_2O), we predict that dissociation of H_2O into Ga−OH and P−H species is unfavorable by 0.56 (0.28) eV per H_2O in the case of species dissociating on non-neighboring (neighboring) Ga and P surface sites. However, we predict that the fully solvated surface (Θ > 2 ML) dissociates water via a novel pathway, namely, through the Ga−OH_2−OH_2−P bridge. The molecules of H_2O are properly oriented to allow a proton transfer between H_2O and a P atom to occur, giving rise to a Ga−OH−OH_2−H−P structure (Figure 2).

For all multilayers studied (Θ > 2 ML), we predict all of the dissociated structures to be lower in energy than the undissociated case (Figure 3a). The half-dissociated (50%) configuration, in which every other molecule is dissociated, is the most favorable in energy among all the degrees of dissociation studied.

Since such Ga−OH and P−H bonds are also created in the (endothermic) dissociation of isolated H_2O molecules for $\Theta \leq$ 2 ML, it is clear that the direct interactions of dissociated water

dx.doi.org/10.1021/ja3063106 | J. Am. Chem. Soc. 2012, 134, 13600−13603

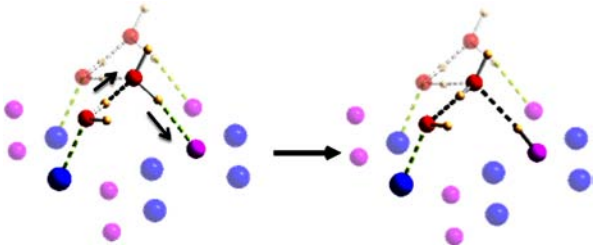

Figure 2. Scheme of the H-bond-mediated dissociation of water on GaP(110). Color code as in Figure 1.

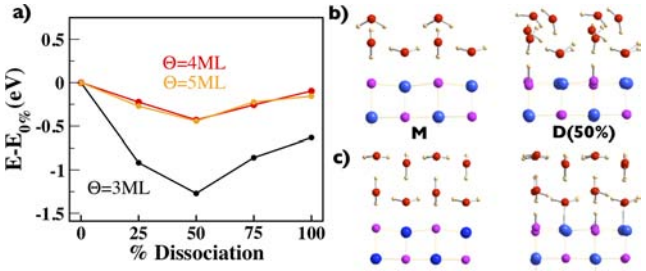

Figure 3. (a) Dissociation energy ($E - E_{0\%}$) of the first water monolayer on GaP(110) as a function of the degree of dissociation for Θ = 3, 4, and 5 ML. (b, c) Structures of the undissociated (M, left) and half-dissociated [D(50%), right] water first layer on GaP(110) for (b) Θ = 3 ML and (c) Θ = 4 ML.

with the surface are not strong enough to induce H_2O dissociation and therefore that H_2O-H_2O interactions come into play. When water molecules are H-bonded, their O−H bonds are weakened, facilitating dissociation. In particular, as it accepts a proton from the surrounding water molecules, the electron density of the H_2O molecule with the H pointing toward P decreases so that proton donation to P is favored.[19,20] For fully solvated surfaces (Θ ≥ 4 ML; see below), our predicted dissociation barrier at half-dissociation is ∼40 meV. The energy profile of the minimum energy path for this process is shown in the SI. This dissociation barrier is only slightly higher than the thermal energy at room temperature ($k_BT \approx 26$ meV). Therefore, we expect water to dissociate spontaneously under ambient conditions. On Zn:GaP, we predict that dissociation is inhibited on Zn sites but also that Zn does not affect the dissociation pattern or the energetics of dissociation occurring on neighboring Ga sites. Thus, 50% dissociation is expected under p-type doping conditions.

Figure 3a also shows a clear dependence of the dissociation energy on the coverage considered. When we compare the distribution of water molecules in the undissociated and dissociated cases for Θ = 3 ML (Figure 3b), we observe that because they are in contact with vacuum, the molecules in the third water monolayer are able to relax their positions freely to accommodate the distortion created by the two first water monolayers in the process of dissociation. Therefore the computed dissociation energy includes not only a component related to the H_2O dissociation itself but also the relaxation energy of those outermost water molecules, as a consequence of the model chosen. However, when higher water coverage is considered (Θ = 4 ML), the model now properly represents a fully solvated surface: the fourth water monolayer prevents artificial relaxation of the third monolayer (Figure 3c), and the computed dissociation energy accounts only for the energy involved in the dissociation process itself. This feature is confirmed by the dissociation energy pattern for Θ = 5 ML. According to these results, the overestimation of the dissociation energy by considering an insufficient water coverage can be as large as 0.84 eV (at 50% dissociation).

After dissociation, the Ga−OH interaction is virtually identical to that between Ga and undissociated OH_2 molecules. In both cases, little change in the Ga−OH/Ga−OH_2 electron density occurs upon adsorption of the half-dissociated water overlayer (Θ = 4 ML; Figure 4). The computed Bader charges

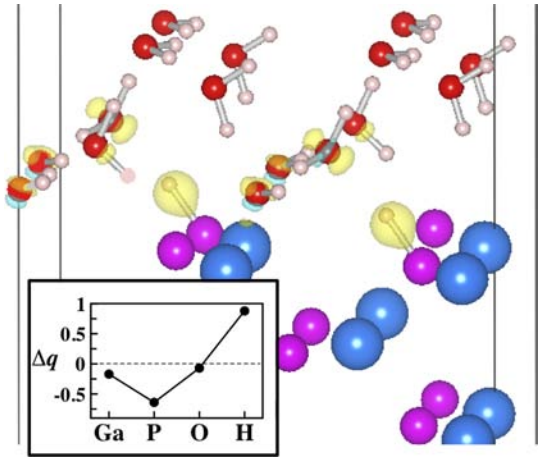

Figure 4. Electron density differences for the interaction between the half-dissociated water slab (Θ = 4 ML) and the GaP(110) surface. Yellow denotes increased electron density and light blue decreased electron density. Isosurface value: 0.02 e/bohr^3. Inset: changes in the Bader charges on the Ga, P, O, and H sublattices per dissociated H_2O upon dissociation (negative indicates loss of electrons, positive indicates gain).

of the oxygen and hydrogen atoms are −1.25*e* and +0.62*e*, respectively, in both the adsorbed OH and OH_2 species. Comparison of these charges with those in isolated H_2O (q_O = −1.20*e*, q_H = +0.60*e*) shows that no charge transfer occurs other than a slight polarization upon adsorption. However, these charges suggest a heterolytic dissociation of H_2O, given the overall charge on adsorbed OH is −0.60*e*. Analogous ionic dissociation of water was reported by Shen and co-workers in similar studies of the III−V semiconductor $(10\bar{1}0)$ GaN surface.[21] With this feature in mind, the interaction cannot be described as covalent but rather as a donor−acceptor/electrostatic one between the electron-deficient surface Ga and electron-rich O atoms. We further find that the positive character of Ga sites increases upon water dissociation (from q_{Ga} = +0.73*e* in the bare surface to q_{Ga} = +0.88*e* at the solvated/half-dissociated GaP/H_2O interface). However, below we show that this change is due to the formation of P−H bonds and not to the new presence of OH species. Nevertheless, this effect enhances the above-mentioned Ga(δ+)/O(δ−) interaction.

Proton donation from H_2O to P creates new P−H bonds that have the same length as those in PH_3 (1.42 Å).[22] These P−H bonds have donor−acceptor character, as shown in Figure 4 by the significant increase in electron density in the P−H region.

The formation of such P−H bonds constitutes a significant change in the chemical features of the solvated GaP surface. The computed Bader charges of adsorbed H show a net gain of ∼0.9*e* per transferred H after formation of the P−H bond (Figure 4, inset), which turns a water hydrogen atom with δ+

dx.doi.org/10.1021/ja3063106 | J. Am. Chem. Soc. 2012, 134, 13600−13603

character (q_H = +0.60e) into a hydride-like species with $q_H \approx -0.3e$ at the GaP surface. The adjacent P atom acts as the major charge supplier, giving ~0.7e via its lone pair. A cooperative effect is observed involving surface Ga atoms, which lose ~0.15e. All of the O atoms in contact with the surface are essentially spectators in this charge rearrangement since they only lose ~0.05e. Thus, the GaP surface becomes an electron-deficient entity in contact with water, and therefore the molecular recognition pattern of the surface may change to one with a strong affinity for electron-donating molecules (e.g., pyridine). Moreover, the hydride-like surface H opens up the possibility of a hydride-mediated scenario for the CO_2 reduction mechanism on GaP electrodes. Indeed, surface metal hydrides have been proposed in the recent literature as possible catalytic agents for activation of CO_2.[23] We suggest that this surface species must be considered when probing the pyridine/CO_2/GaP system and the corresponding CO_2 reduction mechanism.

In conclusion, we have studied the structural and electronic properties of the GaP(110)/H_2O interface by means of first-principles DFT calculations. We find that it is necessary to model a GaP slab solvated by at least four layers of water molecules to obtain a proper description of the structure and energetics of such a solid/liquid interface. Our results show that the solvated GaP(110) surface possesses chemical features beyond a simple superposition of a water layer in contact with a semiconductor. In particular, hydride-like H atoms are predicted to be bound to surface P atoms as a result of partial dissociation of the monolayer of water in contact with the surface. Concomitantly, surface Ga and P atoms are predicted to be electron-deficient, suggesting that electron-donating molecules such as pyridine may adsorb strongly. The interaction of pyridine with a solvated GaP surface is currently under investigation. On the basis of these results, we suggest that the GaP(110) surface should be considered electrochemically active, and thus, its role, and that of adsorbed hydride, must be considered in the mechanism of CO_2 reduction.

■ ASSOCIATED CONTENT

Supporting Information

Further calculation details, results for Zn surface segregation, structural features of the clean GaP(110) and Zn:GaP(110) surfaces, comparison of dissociation patterns on GaP(110) and Zn:GaP(110) surfaces, energy profiles of the water dissociation reaction on GaP(110), and Cartesian coordinates and energies of species discussed in the text. This material is available free of charge via the Internet at http://pubs.acs.org.

■ AUTHOR INFORMATION

Corresponding Author

eac@princeton.edu

Notes

The authors declare no competing financial interest.

■ ACKNOWLEDGMENTS

This work was funded by the Air Force Office of Scientific Research through the MURI Program under AFOSR Award No. FA9550-10-1-057. The authors thank Dr. John A. Keith and Dr. Michele Pavone for helpful discussions.

■ REFERENCES

(1) Benson, E. E.; Kubiak, C. P.; Sathrum, A. J.; Smieja, M. *Chem. Soc. Rev.* **2009**, *38*, 89 and references therein.
(2) Barton, E. E.; Rampulla, D. M.; Bocarsly, A. B. *J. Am. Chem. Soc.* **2008**, *130*, 6342.
(3) Barton Cole, E.; Lakkaraju, P. S.; Rampulla, D. M.; Morris, A. J.; Abelev, E.; Bocarsly, A. B. *J. Am. Chem. Soc.* **2010**, *132*, 11539.
(4) Seshadri, G.; Lin, C.; Bocarsly, A. B. *J. Electroanal. Chem.* **1994**, *372*, 145.
(5) Morris, A. J.; McGibbon, R. T.; Bocarsly, A. B. *ChemSusChem* **2011**, *4*, 191.
(6) Keith, J. A.; Carter, E. A. *J. Am. Chem. Soc.* **2012**, *134*, 7580.
(7) Tossell, J. A. *Comput. Theor. Chem.* **2012**, *977*, 123.
(8) Blochl, P. *Phys. Rev. B* **1994**, *50*, 17953.
(9) (a) Hohenberg, P.; Kohn, W. *Phys. Rev.* **1964**, *136*, B864. (b) Kohn, W.; Sham, L. J. *Phys. Rev.* **1965**, *140*, A1133.
(10) Perdew, J. P.; Burke, K.; Ernzerhof, M. *Phys. Rev. Lett.* **1996**, *77*, 3865.
(11) (a) Kresse, G.; Hafner, J. *Phys. Rev. B* **1993**, *48*, 13115. (b) Kresse, G.; Furthmüller, J. *Phys. Rev. B* **1996**, *54*, 11169. (c) Kresse, G.; Furthmüller, J. *Comput. Mater. Sci.* **1996**, *6*, 15.
(12) *Semiconductors: Group IV Elements and III−V Compounds*; Madelung, O., Ed.; Data in Science and Technology Series; Springer: Berlin, 1991.
(13) Monkhorst, H. J.; Pack, J. D. *Phys. Rev. B* **1976**, *13*, 5188.
(14) (a) Bader, R. F. W. *Atoms in Molecules: A Quantum Theory*; Oxford University Press: New York, 1990. (b) Tang, W.; Sanville, E.; Henkelman, G. *J. Phys.: Condens. Matter* **2009**, *21*, No. 084204.
(15) Webb, C.; Lichtensteiger, M. *J. Vac. Sci. Technol.* **1982**, *21*, 659.
(16) Henrion, O.; Löher, T.; Klein, A.; Pettenkofer, C.; Jaegermann, W. *Surf. Sci.* **1996**, *366*, 1685.
(17) Henkelman, G.; Uberuaga, B. P.; Jónsson, H. *J. Chem. Phys.* **2000**, *113*, 9901.
(18) (a) Fishwick, L.; Walker, M.; Bradley, M. K.; Woodruff, D. P.; McConville, C. F. *Phys. Rev. B* **2012**, *85*, No. 045322. (b) Alvés, J. L. A.; Hebenstreit, J.; Scheffler, M. *Phys. Rev. B* **1991**, *44*, 6188. (c) Swarts, C. A.; McGill, T. C.; Goddard, W. A., III. *Surf. Sci.* **1981**, *110*, 400.
(19) Huš, M.; Urbic, T. *J. Chem. Phys.* **2012**, *136*, 144305.
(20) Bartha, F.; Kapuy, O.; Kozmutza, C.; Van Alsenoy, C. *THEOCHEM* **2003**, *666−667*, 117.
(21) (a) Shen, X.; Allen, P. B.; Hybertsen, M. S.; Muckerman, J. T. *J. Phys. Chem. C* **2009**, *113*, 3365. (b) Shen, X.; Small, Y. A.; Wang, J.; Allen, P. B.; Fernández-Serra, M. V.; Hybertsen, M. S.; Muckerman, J. T. *J. Phys. Chem. C* **2010**, *114*, 13695.
(22) Sennikov, P. G. *J. Phys. Chem.* **1994**, *98*, 4973.
(23) Kumar, B.; Llorente, M.; Froehlich, J.; Dang, T.; Sathrum, A.; Kubiak, C. P. *Annu. Rev. Phys. Chem.* **2012**, *63*, 541.